

Review of Correlation Data:
Departures from the Statistical Model*
S. F. Mughabghab
Brookhaven National Laboratory

ABSTRACT

γ-ray spectra due to radiative neutron capture in the thermal and resonance region are examined for nonstatistical effects. The data appears to be consistent with the interpretation that generally direct hard sphere capture dominates in the thermal region for $A < 46$ while valence capture plays a significant and sometimes dominant role in the vicinity of the peaks of the 2P, 3S and 3P single particle giant resonances. Additional evidence of valence capture is provided by data on ^{24}Mg , ^{36}Ar , and ^{54}Fe . On the other hand, correlations between partial radiative widths and either the (d,p) spectroscopic factors or the reduced neutron widths are reported. Since the magnitude of the valence neutron contribution cannot account for these observations, the doorway state picture is invoked.

I. INTRODUCTION AND DEVELOPMENT

The interaction of low energy neutrons with nuclei forms highly excited narrow resonant states just above the neutron separation energy. Because of the extreme complexity of the initial capturing states the radiative decay amplitudes are randomly distributed with zero mean. In other words, the radiative widths for a single channel follow the Porter Thomas distribution. It is now generally recognized that these highly excited states conform to a description in terms of the statistical model. This picture proved to be very successful, for example, in the determination of spins of initial as well as final states. However, accumulating experimental evidence derived from neutron capture data indicates that nonstatistical effects, particularly in the mass region from $A=24$ to 142, play a major and sometimes dominant role in s- and p-wave neutron capture. Recently, the subject of nonstatistical effects was reviewed by Lane⁽¹⁾ and by Mughabghab⁽²⁾ and the thermal capture data analyzed and interpreted by Kopecky,

*Work supported by the U. S. Atomic Energy Commission

MASTER

NOTICE
This report was prepared as an account of work sponsored by the United States Government. Neither the United States nor the United States Atomic Energy Commission, nor any of their employees, nor any of their contractors, subcontractors, or their employees, legal liability, warranty, express or implied, or assumes any responsibility for the accuracy, completeness or usefulness of any information, apparatus, product or process disclosed, or represents that its use would not infringe privately owned rights.

fy

Spits, and Lane^(3,4).

This survey attempts to describe our present understanding of non-statistical effects in radiative neutron capture in the thermal and resonance regions in terms of simple reaction mechanisms. Some of these simple reaction mechanisms are: (1) direct or hard sphere capture, (2) channel capture of Lane and Lynn⁽⁵⁾ or valence neutron model of Lynn⁽⁶⁾ and (3) the semi direct capture of Brown⁽⁷⁾ or doorway state formation of Estrada and Feshbach⁽⁸⁾. The doorway state picture as applied specifically to (n, γ) reaction was theoretical developed by Lane⁽⁸⁾ and Beer⁽¹⁰⁾.

Potential or Hard Sphere Capture

The hard sphere or potential capture cross section for a neutron undergoing a transition from an initial s state to a final p state is expressed by: (5)

$$\sigma (\text{hard sphere}) = \frac{0.062}{R} \frac{Z}{A} k_n^2 \left(\frac{Z}{A} \right)^2 \theta_n^2 y^2 \left(\frac{y+3}{y+1} \right)^2 \quad (1)$$

where R is the effective hard sphere radius in fm, θ_n is a dimensionless reduced neutron width of the final state and $y = k_{NL} R$ where k_{NL} is the wave number corresponding to the binding energy of the final state. This relationship exhibits two interesting features:

(i) The partial capture cross section (or reduced γ ray intensities) are correlated with the (d,p) spectroscopic factors of the final state and (ii) the γ ray intensities follow an E_γ energy dependence. One can thus experimentally study direct or hard sphere capture by measuring the γ ray intensities with the view of investigating their energy dependence and their correlation with the (d,p) spectroscopic factors. This is conveniently carried out in the off resonance region and at thermal energies. At this point it is important to note that the numerical magnitude of hard sphere capture is about 0.9b in the vicinity of the 3S single particle giant resonance; and for mass numbers below A=40 it is of the order of a few millibarns⁽⁵⁾.

Valence Capture

By considering the motion of a neutron in a potential-well and by neglecting

core excited processes Lynn derived an expression for the partial electric dipole photon width from an initial state i to a final state f :

$$\Gamma_{\gamma if}(E1) = \frac{16\pi k^3}{9} \theta_i^2 \theta_f^2 (\bar{e} I M_{if})^2 \quad (2)$$

where θ_i^2 and θ_f^2 are dimensionless reduced neutron widths of the initial and final states and are given by $\theta_i^2 = \gamma_{ni}^2 / \gamma_{sp}^2$ and $\theta_f^2 = S_{dp}$. The effective charge of the neutron (\bar{e}) is expressed by $\bar{e} = \frac{-eZ}{A}$. M_{if} and I are the angular momentum vector coupling coefficient and the radial overlap integral respectively. The radial overlap integrals are calculated by Lynn using a Saxon-Woods potential with a spin orbit coupling term. It is important to note that in these calculations, the radial wave functions are normalized throughout space. Recently Lane and Hughesghab derived a corrected expression for valence neutron capture. In this study, it was shown that the wave functions of the single particle states must be normalized inside the nuclear surface. This criterion would then introduce a correction factor to the radial overlap integrals as calculated by Lynn. The normalization procedure for the case of $3p \rightarrow 3s$ transitions is illustrated in Figure 1. The $3p$ single particle initial state is taken

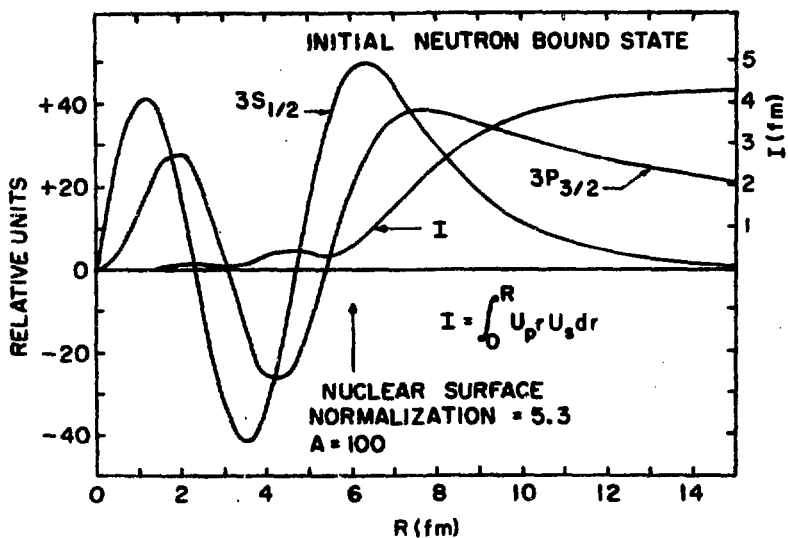


Figure 1

as lightly bound. Applied to mass region $A=100$, the normalization factor is found to be 5.3. In addition, the dependence of the radial overlap integral, I , with distance is shown. Note that most of the contribution to I is arising from the region outside the nuclear surface. The interesting feature of this normalization procedure is that as the binding of the initial neutron state increases the normalization factor decreases with a corresponding decrease in the valence capture contribution. This implies that certain mass regions, such as the 3p and 3s single particle giant resonances, will be more favorable to the observation of valence capture than others.

In addition the reduced single particle width γ_{sp}^2 of a realistic potential such as a Saxon-Woods potential should be used. Vogt⁽¹²⁾ has demonstrated that this is expressed by:

$$\gamma_{sp}^2 = \frac{\hbar^2}{ma^2} (1 + 6.7 d^2) \quad (3)$$

where d is the diffuseness of the nuclear surface. The success of the valence neutron model in the 3p giant resonance particularly in ⁹⁸Mo and ⁹⁶Zr raised two theoretical problems (1) why p→s, d and s→p transitions are decoupled from the giant dipole resonance and (2) why excited target states do not contribute? These problems have been examined by Lane¹⁴ and Gyarmati et al¹⁵ and solutions have been proposed.

At this stage it should be pointed out that Boridy and Mahaux¹⁶⁻¹⁷ investigated valence capture in the framework of the shell model of nuclear reactions and derived expressions for the partial photon width. These will be discussed by Dr. Mahaux in his talk.

Because of the previous discussion, the radiative decay amplitude for the neutron resonant state is expressed as a sum of various contributions:

$$\begin{aligned} \Gamma_{\gamma if}^{1/2} = & C_1 \Gamma_{\gamma if}^{1/2} (HS) \sigma + C_2 \Gamma_{\gamma if}^{1/2} (CV) + C_3 \Gamma_{\gamma if}^{1/2} (DS) \\ & + C_4 \Gamma_{\gamma if}^{1/2} (CN) \end{aligned} \quad (4)$$

where the terms on the right hand side correspond to contributions of hard sphere capture, valence or channel capture, doorway state contribution and compound nucleus formation respectively. It is the purpose of this investigation to explore the experimental data and attempt to find out in what mass regions single particle effects dominate.

Since the title of this paper is Review of Correlation Data, it is appropriate at this stage to define the linear correlation coefficient of two variables x_1, y_1 ,

$$\rho = \frac{\sum_1 (x_1 - \bar{x}_1) (y_1 - \bar{y}_1)}{\left[\sum_1 (x_1 - \bar{x}_1)^2 \sum_1 (y_1 - \bar{y}_1)^2 \right]^{1/2}} \quad (5)$$

where

$$x_1 = (2J+1) S_{dp} \text{ for s-wave capture}$$

$$y_1 = \frac{\Gamma_{\gamma 1}}{E \gamma^n} \cdot \gamma_n^2$$

\bar{x}_1 and \bar{y}_1 are the mean values

The power appearing in the γ ray energy will be referred to as the reduction factor. Now let us turn our attention to the capture data to examine its nonstatistical aspects as reflected in the observation of significant correlation coefficients between various channels. I would like to divide the experimental data into three parts dealing with hard sphere, valence, and doorway state capture.

II. Thermal Capture Data or

the Question of Direct Versus Valence Capture

Direct Capture: Evidence from Thermal Data

Some time ago it was noted by Groshev and Collaborators⁽¹⁸⁾ that there is a significant correspondence between reduced γ ray intensities and (d,p) spectroscopic factors in thermal neutron capture γ rays for the following target nuclei: ^{24}Mg , ^{28}Si , ^{32}S , and ^{40}Ca . Such and similar observations have been theoretically investigated by Lane and Wilkenson¹⁹ and later by Bockelman²⁵ in

terms of the concept of parantage of nuclear states. A detailed and exhaustive comparison between theory and experiment was not possible at the time because of lack of adequate and reliable (n, γ) and (d,p) data. With the availability of intense neutron sources and highly enriched samples, particularly for isotopes with low natural abundance, a wealth of thermal capture data is presently available. Figure 2 presents a summary of the experimental data for the even-even target nuclei, $^{24,26}\text{Mg}$, $^{28,30}\text{Si}$, $^{32,34}\text{S}$, $^{36,40}\text{Ar}$, $^{40,42,44,46,48}\text{Ca}$, $^{50,52,54}\text{Cr}$, $^{60,62}\text{Ni}$. Two strongest γ rays populating final p states with large S_{dp} are considered. In most cases these states happen to be the $p_{1/2}$ and $p_{3/2}$ components of the single particle p state. The experimental ratio of the intensities is found and this is compared with a calculated ratio based on the relation $I_\gamma \propto (2J+1) E_\gamma^n$, where n is assumed to be 1, 2, 3 at the top, center and bottom of Figure 2 respectively. With the exception of ^{42}Ca , $^{50,52}\text{Cr}$ and possibly ^{54}Cr ,

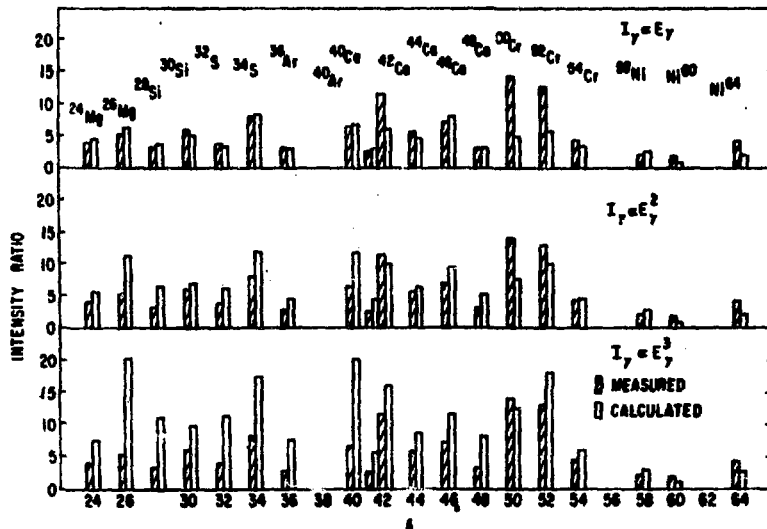


Figure 2

the agreement is reasonably good for the majority of cases when a reduction factor, $n = 1$, is considered. On the other hand for $^{50,52,54}\text{Cr}$ agreement between measurements and calculations is considerably improved for a reduction

factor $n = 2.5$. These features of the experimental data (i) small cross section of the nuclei and (ii) the E_y energy dependence indicate that hard sphere capture is the dominant reaction mechanism in the mass region $A < 50$. A detailed method of analyzing nonstatistical effects is the study of the variation of the correlation coefficient ρ (S_{dp} , $I_{y_{1j}} / E_y^n$) with the reduction factor n . The RCN group devoted considerable effort to this type of investigation. Similar type of analysis is carried out⁽²¹⁾ for the following nuclei $^{50,54}\text{Cr}$, ^{48}Ti , and ^{54}Fe and this is shown in Figure 3. As noted, the correlation coefficient is optimized for an

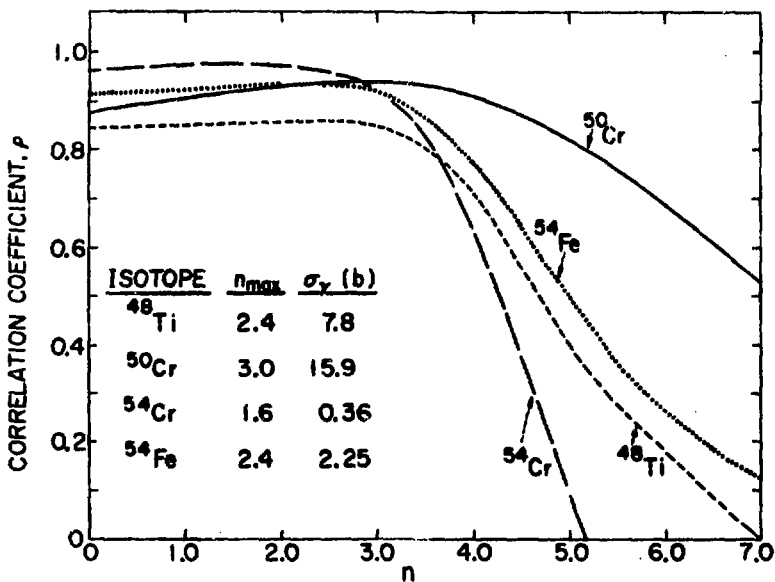


Figure 3

n in the range 2-3. This feature is indicative of channel or valence neutron capture, which will be discussed in the next section.

Most even-odd target nuclei with target spin I do not exhibit strong correlation coefficients. This is due to the fact that two channel spins $l + \frac{1}{2}$ and $l - \frac{1}{2}$ are available for s -wave capture. If both of these channel spins contribute, then the correlation coefficient is reduced⁽²²⁾ by a factor $\sqrt{2}$ relative to the case for target nucleus with spin 0. However the pioneering investigations of Spits et al⁽²³⁾ showed that the correlation coefficient

approaches unity for $n = 1.2$. This was interpreted by Kopechy, Spits and Lanc⁽⁴⁾ in the framework of direct capture. Other odd-even target nuclei which are good candidates of hard sphere capture are ^{27}Al , ^{37}Cl , ^{39}Si , ^{31}P and possibly ^{49}Ti . Figure 4 illustrates the variation of the correlation coefficient with the reduction factor for these nuclei. Note that the correlation coefficient

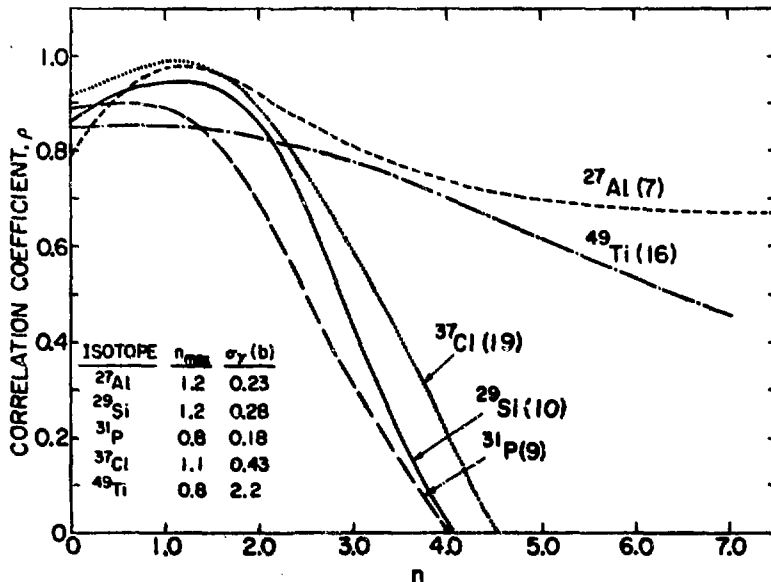


Figure 4

for these nuclei approaches unity for $n = 1$. This information when combined with the small capture cross sections of these nuclei, which is about the magnitude predicted by direct capture, indicates that the capture process is not a resonance phenomenon and can be interpreted in terms of hard sphere capture. However, ^{49}Ti requires special attention. Note that the known positive energy resonance of ^{49}Ti contribute 1.16b to the thermal capture cross section out of a total measured capture cross section of 2.2 ± 0.3 b.

Additional measurements of thermal capture data by Mariscotti et al⁽²⁵⁾ and Groshev et al⁽²⁶⁾ showed that nonstatistical effects are not restricted to the mass region of the 38 giant resonance. The results of Mariscotti et al⁽²⁵⁾

showed that a high and significant correlation coefficients exist between the (n,γ) and (d,p) reactions for ^{138}Ba , ^{142}Nd , ^{140}Ce . This was interpreted in terms of the common unique parent assumption of Lane and Wilkenson.⁽¹⁹⁾ The data in this mass region is compiled and an analysis⁽²¹⁾ similar to that carried out for the light mass region is carried out here (Figure 5). In order to shed

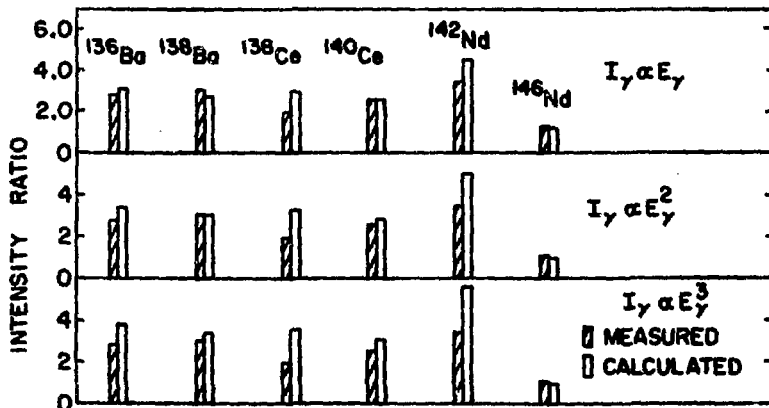


Figure 5

further light on the reaction mechanism in this mass region a study of the dependence of correlation coefficient on the reduction factor is carried out. Of those nuclei, only ^{138}Ba is studied extensively by (d,p) reactions for the purpose of deriving spectroscopic factors over a broad region of excitation energy. Detailed study⁽²¹⁾ of the correlation coefficient for ^{138}Ba shows that ρ is maximized for $n = 1.6$, thus suggesting hard sphere capture plays a dominant role. On the other hand the large thermal cross section of ^{142}Nd ($\sigma_\gamma = 18.7 \pm .7b$) makes it difficult to interpret the ^{142}Nd thermal capture data in terms of hard sphere capture. The parameters of a bound level are extracted⁽²¹⁾ in order to assess the importance of valence neutron capture. The results of the analysis show that valence neutron contribution is not sufficiently large to account for the observed data. Possibly more complex reaction mechanisms such as doorway state contribution are required here.

It is interesting to compare the ^{138}Ce data with that of ^{136}Ba . Spectro-

scopic factors for ^{139}Ce are not yet determined. However since both of these nuclei contain 81 neutrons it would be expected that S_{dp} of the levels of ^{139}Ce at 2509 and 1971 keV are similar to those of ^{137}Ba at 2179 and 2646 keV (Figure 6).

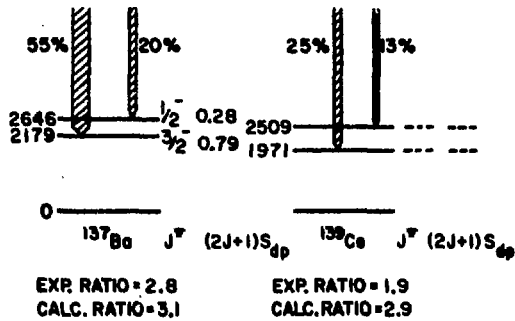


Figure 6

On the basis of this assumption, one calculates an intensity ratio of 2.9. This is to be compared to an experimental ratio of 1.9. It must be noted that spectroscopic data for ^{139}Ce is required in order to confirm these results.

The summary of the experimental data in the mass region from ^{27}Al to ^{66}Zn is illustrated in Figure 7, where n_{max} is plotted versus the atomic number. We note that an interesting general trend emerges from this study. The data seems to fall into three groups characterized by $n=1.1, 2.4,$ and 4.8 . It is tempting to interpret this trend as a change of the reaction mechanism for s-wave neutron capture with mass number. In the mass region from ^{24}Mg to ^{46}Ca , hard sphere capture which is characterized by $n_{\text{max}} = 1.1$ dominates. As we proceed to the mass region comprising Ti, Cr, Fe Ni isotopes valence or channel capture ($n_{\text{max}} = 2-3$) plays a dominant role and finally at mass numbers above ^{64}Ni both of these single particle components diminish and the influence of the giant dipole resonance sets in. These observations are consistent with theoretical expectations which show that the "direct" and valence components peak at $A = 45$ and 55 respectively.

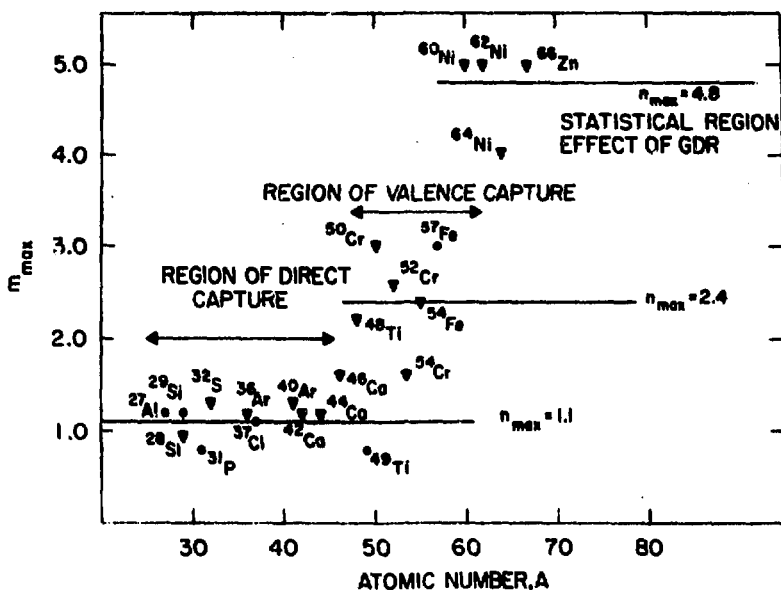


Figure 7

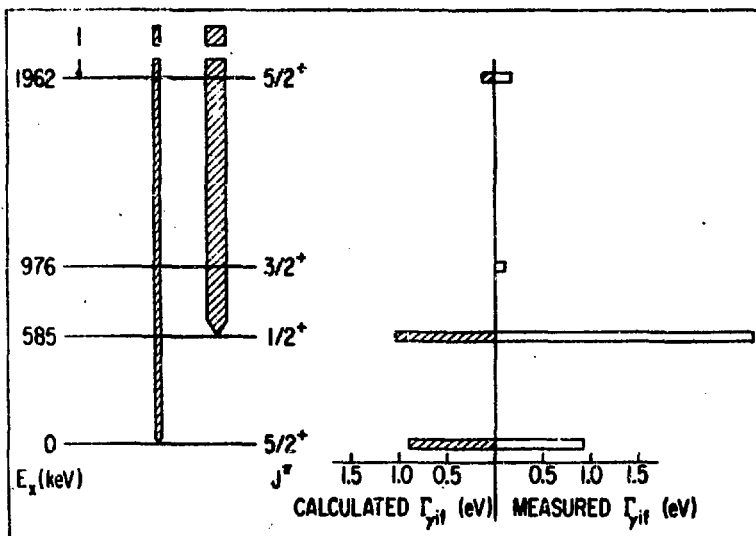
III EVIDENCE OF VALENCE CAPTURE

Now let us turn our attention to the resonance capture data with the view of discussing valence neutron capture in the 2p, 3s, 3p giant resonances.

(1) 2p Giant Resonance:

The neutron single particle 2p state is located above the neutron separation energy at about $A=30$. Resonance neutron capture in ^{24}Mg provides us with the best illustration of the importance of valence neutron capture in this mass region. The neutron resonances of ^{24}Mg at 83, 263, and 430 keV are known to be extraordinarily strong p-wave resonances. Since data on radiative transitions in the 83 keV resonance are available from both neutron capture²⁷ and threshold photoneuclear reactions,²⁸ calculations of partial radiative widths due to neutron capture in this resonance are carried out by Mughabghab²⁹ in the framework of the valence neutron model. Since a strong transition to

the $d_{5/2}$ ground state of ^{25}Mg is observed, the spin of the 83 keV resonance is $3/2$. Therefore the important valence neutron transitions here are $p_{3/2} \rightarrow d_{5/2}$ and $p_{3/2} \rightarrow s_{1/2}$. Note that the weak transition to the $d_{3/2}$ state of ^{25}Mg at $E_x = 976$ keV may give a signature of valence neutron capture. This is due to the fact that the angular momentum vector coupling coefficient for a $p_{3/2} \rightarrow d_{3/2}$ transition is reduced by a factor of 9 relative to a $p_{3/2} \rightarrow d_{5/2}$ transition. The results are presented in Figure 8 and are compared with measurements of Bergqvist et al.²⁷ In deriving the measured radiative widths from the intensity values, a correction due to the γ -ray angular anisotropy is made, and a total radiative width of 5 ± 1 eV was adopted from the experimental data. As shown, the agreement between the predictions ($\Gamma_{\gamma if} = 0.93$ eV) and measurements ($\Gamma_{\gamma if} = 0.90$ eV) is remarkably good for the ground state transition $p_{3/2} \rightarrow d_{5/2}$. The threshold photoneutron result is $\Gamma_{\gamma if} = 1.1$ eV for this transition. On the other hand, the partial radiative width for the $p_{3/2} \rightarrow s_{1/2}$ transition is enhanced by a factor of 2.6 over the predictions of the model.



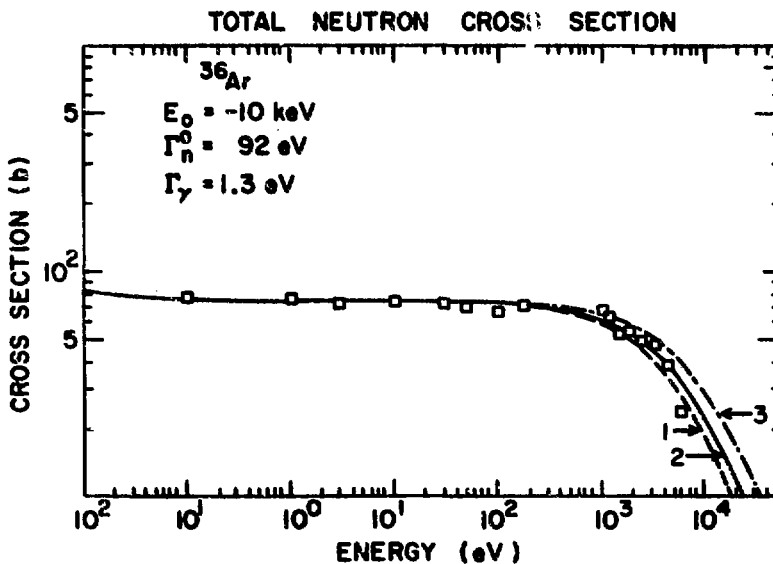
RADIATIVE p-WAVE NEUTRON CAPTURE IN 83-keV RESONANCE OF Mg^{24}

Figure 8

In this mass region, Jackson and Toohay⁽³⁰⁾ using the (γ, n) reaction measured the ground state radiative widths of ^{29}Si resonances in the energy range 175-1315 keV. A correlation coefficient $\rho(\Gamma_{\gamma\text{if}}, \gamma_n^2) = 0.88$ is reported. This is attributed to doorway state contributions. Allen and Macklin reported total radiative widths for ^{28}Si . Their data indicate that there is a suggestion of a correlation between Γ_γ and γ_n^2 for p-wave resonances.

(ii) 3S Giant Resonance

Below the 3S giant resonance, thermal capture data of ^{36}Ar provides us with a good example of the dominant role of valence neutron capture. A capture cross section of 5b and a coherent scattering amplitude of +73.7b, indicate that the thermal capture spectra of ^{36}Ar are dominated by the effect of a strong bound s-wave resonance. It is therefore necessary to determine its parameters which are required in the calculation of partial radiative widths in the framework of the valence neutron model. This is achieved by carrying out a parametric fit to the total cross section⁽³²⁾ (Figure 9) which is renormalized to the recommended values of σ_γ and σ_n .⁽²⁴⁾ Note that the



shape of the cross section in the keV region determines reasonably well the position and hence accurately the parameters of the bound level. A display of the energy level diagram of ^{36}Ar and the γ ray intensities due to thermal neutron capture as measured by Von Wille⁽³³⁾ are shown in Figure 10. One

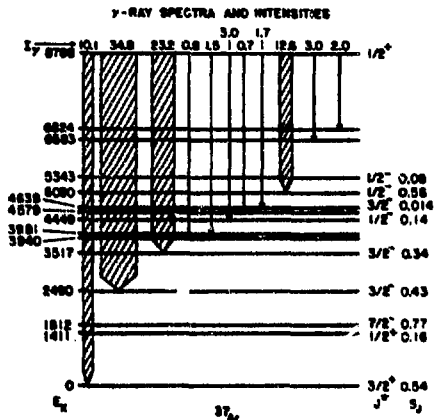


Figure 10

immediately recognizes that E1 transitions feeding final p states are strongly correlated with the (d,p) data. In view of this the partial radiative widths are calculated in the framework of the valence neutron model. A comparison between measured and predicted partial radiative widths is displayed in Figure 11 which demonstrates the remarkable agreement between the two sets. It is interesting to point out that a detailed analysis⁽²¹⁾ of the ^{36}Ar γ ray intensities shows that ρ is optimized for $n_{\text{max}} = 1.2$, a result which cannot be understood in terms of channel or valence capture for which $n_{\text{max}} = 2-3$. At the peak of the 3S giant resonance ^{50}Cr and ^{58}Ni were presented previously as good candidates for valence capture.^(2,34) Here we report ^{54}Fe as another candidate for valence capture. As shown in the previous discussion, $n_{\text{max}} = 2.4$ for the thermal intensities of ^{54}Fe , implying valence or channel effects. Analysis in terms of the positive neutron energy resonances of ^{54}Fe indicates that ^{54}Fe thermal cross section is accounted for largely in terms of the 7.8 keV resonance; and as a result the radiative width for this resonance is 2.4 eV. Because of this

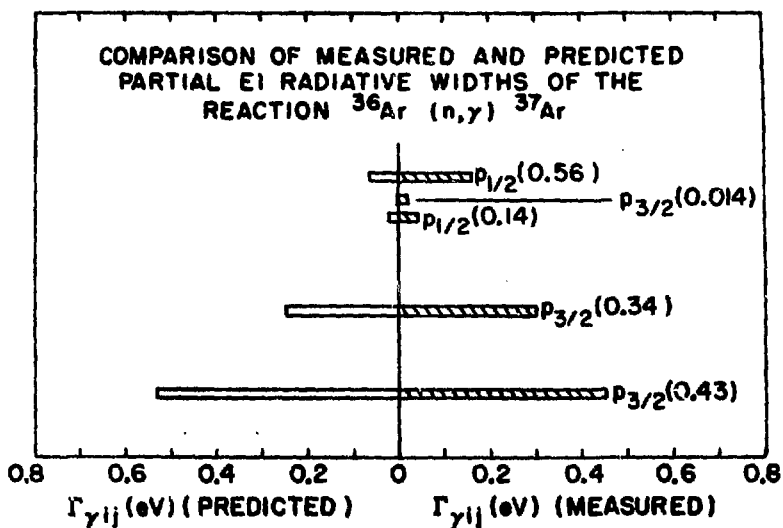


Figure 11

information and neglecting interference effects, the thermal γ ray intensities provide a representation of the capture spectra of the 7.8 keV resonance of ^{56}Fe . In Figure 12, the energy level diagram and γ ray intensities⁽²⁵⁾ of ^{55}Fe are represented on the left hand side. A comparison of the measured partial radiative widths is made with the calculated values in the framework of the valence neutron model. As demonstrated in Figure 12, valence neutron transitions play a dominant role.

Measurements of total radiative widths with a large liquid scintillator by Stieglitz et al³⁶ and Spencer and Beer³⁷ showed that the total radiative widths of s-wave resonances are correlated with their reduced neutron widths for the Ti, Cr, Fe and Ni isotopes. For 40 resonances of the even-even nuclei $\rho(\Gamma_{\gamma i}, \Gamma_{ni}^0) = 0.4 \pm 0.10$ with 1.6% probability that this value could occur randomly.³⁷

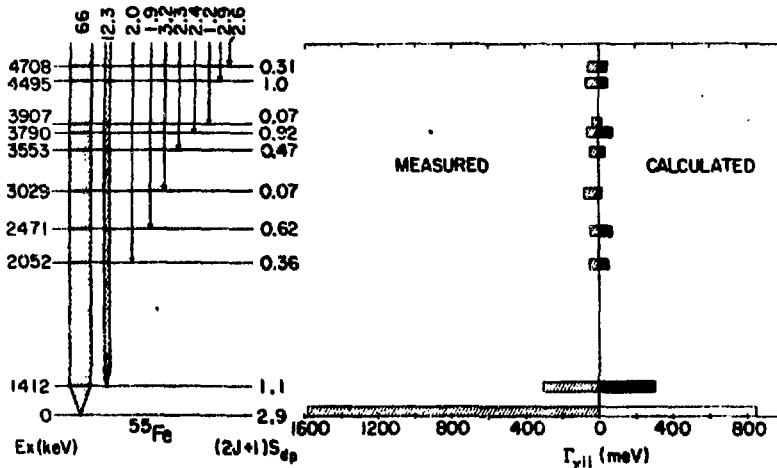


Figure 12

(iii) 3p Giant Resonance:

The best evidence of the importance of valence neutron capture was initially provided by the investigations of Mughaghab et al^{2,13} in the mass region spanning the 3p giant resonance. At the peak of the 3p giant resonance, ⁹⁸Mo and ⁹⁶Zr p-wave capture data best exemplifies the dominant role of valence neutron capture. Figure 13 describes the γ ray spectra due to neutron capture in the 302 eV p-wave resonance of ⁹⁶Zr. The strong γ ray with energy 5572.1 keV populates the ground state of ⁹⁷Zr, which is characterized as a pure single particle state. The bottom of Figure 13 shows the remarkable agreement between predicted and measured partial radiative widths.

The γ ray spectra due to p-wave neutron capture in the neutron resonances of ⁹⁸Mo at 12, 429, 612 and 818 eV resonances are described in Figure 14. The striking similarity of the 429 and 612 eV resonances is at variance with the statistical model. This feature suggests that the nuclear structure properties of these two resonances are quite similar. Note that γ ray transitions in the s-wave resonance are not enhanced. Figure 15 illustrates the dominance of valence neutron p-wave capture in ⁹⁸Mo resonances at 12, 429, 612, 818, and 2700eV.

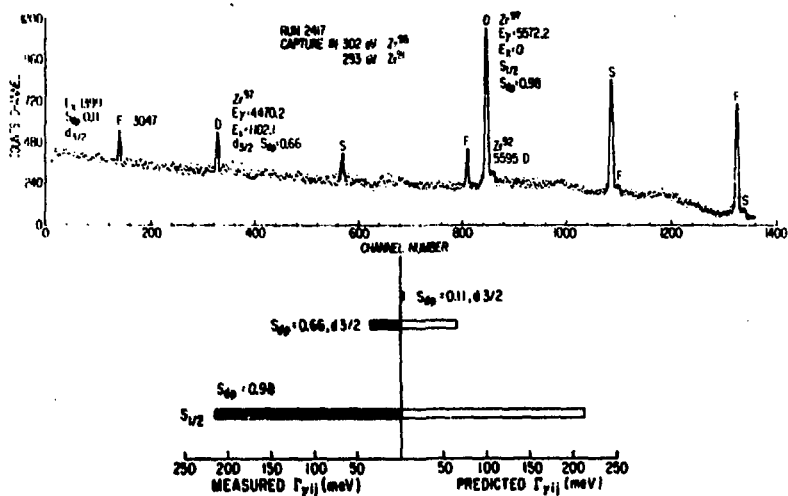


Figure 13

On the other hand the comprehensive investigations of Wasson and Slaughter⁽³⁸⁾ carried out for 16 p-wave resonances of ⁹²Mo showed that valence neutron capture plays a significant but not as dominant a role as in ⁹⁸Mo. Wasson and Slaughter⁽³⁸⁾ reported a correlation coefficient of 0.51 for the p-wave resonances for the 7126keV γ ray populating the first excited $s_{1/2}$ state of $E_x = 942$ keV. This correlation coefficient is largely due to the large reduced width of the 23.9 keV resonance. It is interesting to note that other γ rays corresponding to transitions to $d_{3/2}$ and $d_{5/2}$ final states do not exhibit any correlation with the initial capturing state.

To study the correlation of $\Gamma_{\gamma ij}$ with the spectroscopic factors of the final states, an averaging of the partial radiative widths for four $p_{1/2}$ and twelve $p_{3/2}$ resonances is carried out. The variation of the correlation coefficient with the reduction factor, n , is illustrated in Figure 16. Note that for an E_γ^3 energy dependence of the partial radiative widths, $p_{1/2}$ and

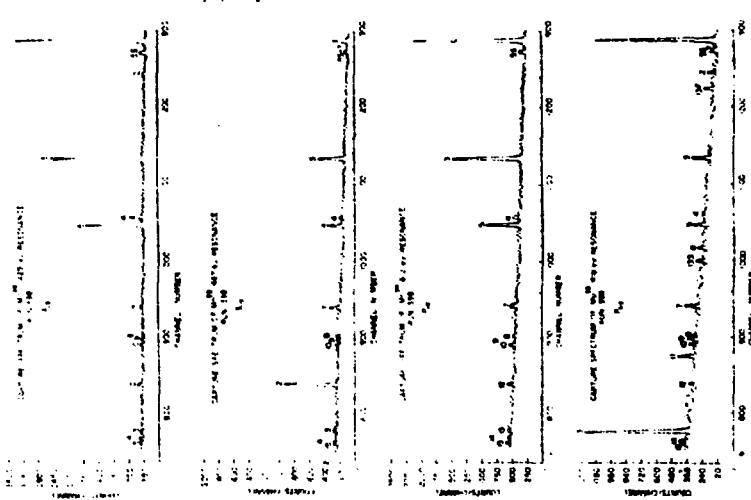


Figure 14

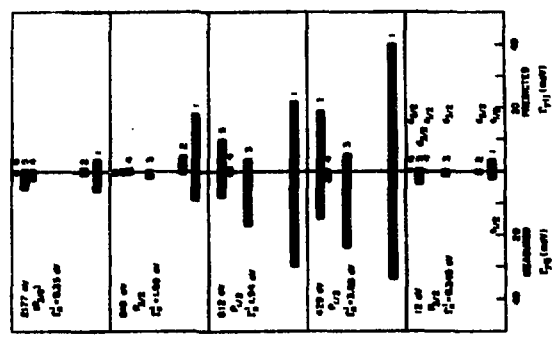


Figure 15

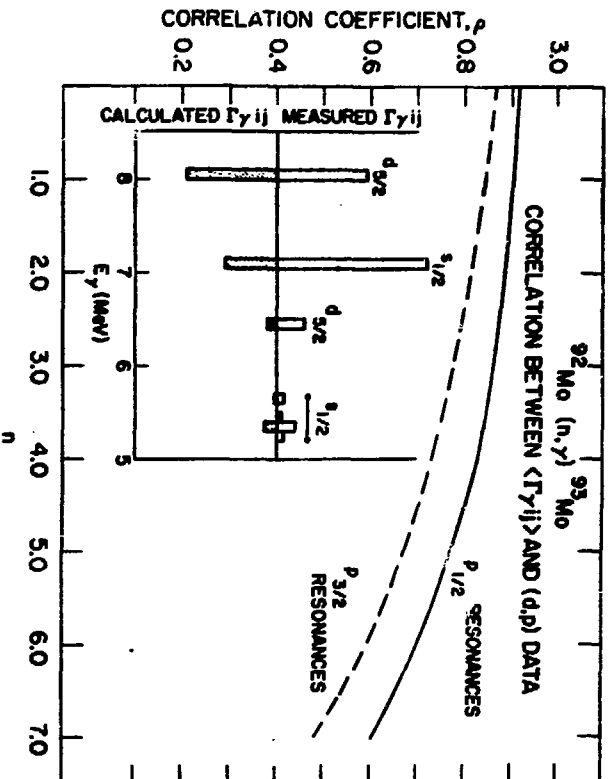


Figure 16

$p_{3/2}$ resonances exhibit significant correlation coefficients 0.83 and 0.77 respectively. In these calculations the angular momentum spin factors and radial overlap integrals have been taken into account in terms of Equation 2. In the inset to Figure 16, a comparison between measurements and calculations is carried out for the case of $p_{3/2}$ resonances. The $d_{3/2}$ final states were not included in the comparison since $p_{3/2} \rightarrow d_{3/2}$ transitions are inhibited in the valence neutron model. Note that the transition populating the first excited state is enhanced by a factor of about 3. This enhancement can be brought about by invoking a doorway state contribution.

Using a filtered neutron beam, Sismani and Chrien (39) studied the spectra due to neutron capture in the separated isotopes $^{92,98,98}\text{Mo}$. The results of these investigations show that the γ ray intensities are highly correlated with

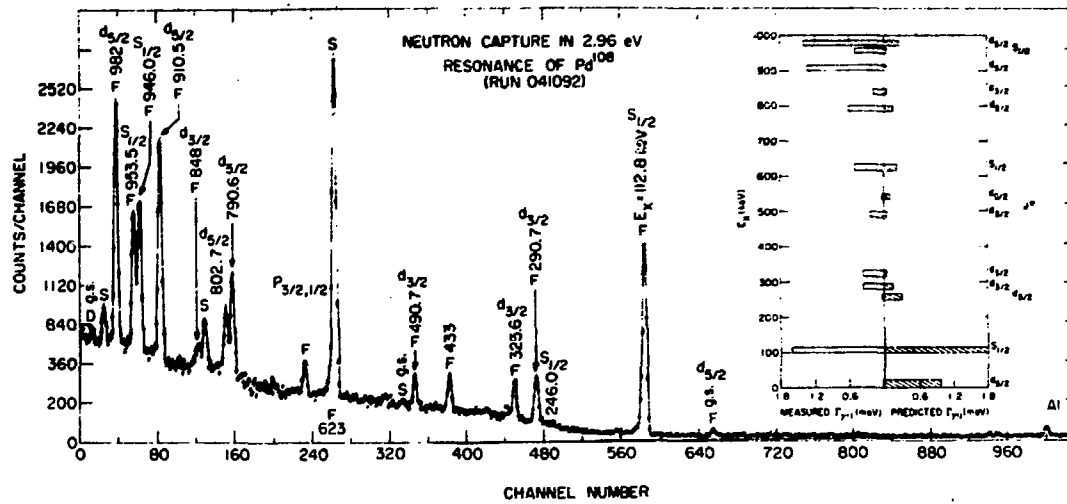


Figure 17

the (d,p) data.

Measurements of capture γ ray spectra from individual resonances of ^{93}Mo have been carried out. A significant correlation coefficient between partial radiative widths and spectroscopic factors is reported for p- but not s-wave resonances. (40) This was interpreted in terms of doorway state contributions.

Additional support for the importance of valence neutron transitions in the 3p giant resonance comes from the threshold photoneutron work of Toohy and Jackson. (41) The (γ,n) reaction was exploited to study the ground state radiative widths of $^{90}\text{Zr} + n$ resonances. In their detailed analysis, Toohy and Jackson show that the valence neutron contribution, in this case for $P_{3/2} \rightarrow d_{5/2}$ transition, is as important as compound nucleus formation.

In p-wave capture in the 2.96 eV resonance of ^{108}Pd , (Figure 17) the transition $P_{3/2} \rightarrow s_{1/2}$ feeding the first excited state of ^{109}Pd is well described (42) by the valence neutron model. In contrast, the transition populating the $d_{5/2}$ ground state seems to be inhibited. The investigations of p-wave neutron capture which were carried out in the 3p giant resonance indicate that valence neutron capture plays an important and sometimes dominant role. The general trend of the data appears to indicate that p \rightarrow s transitions retain their strength better than p \rightarrow d transitions. Additional evidence for this behavior is provided by the γ ray transitions in bound p-levels. Some of the interesting problems raised are the following: can this aspect of the data be explained in terms of the initial and/or final states? Is the structure of the initial state as important as the final state? Additional experimental and theoretical investigation are required in order to shed additional light on this interesting and exciting field of capture γ ray spectroscopy.

(iv) 4S GIANT RESONANCE

As pointed out previously, in the mass region of the 4S giant resonance, the thermal capture data of the Ba, Cs, and Nd isotopes establish a correspondence between the (n, γ) and (d,p) data. The results of ^{138}Ba indicate that hard sphere capture is dominant. However the ^{142}Nd data cannot be interpreted in terms of either hard sphere or valence capture. Possibly

doorway state processes come into play here. The fragmentation of the initial and final single particle states makes the observation of nonstatistical effects a difficult task. The experimental problems associated with this mass region have been pointed out. (2) Many attempts (43-48) were made for a search of possible nonstatistical effects in this mass region. The investigation of the reaction mechanism in $^{173}\text{Yb}(n,\gamma)^{174}\text{Yb}$ have been discussed in detail previously. (2) The results of these investigations are summarized in Figure 18.

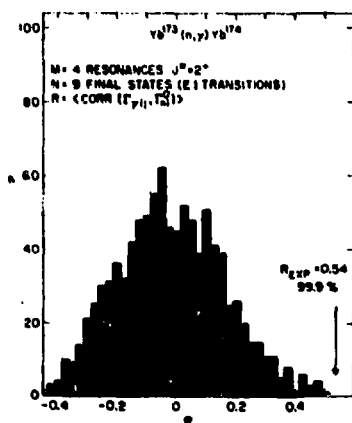


Figure 18

As indicated, analysis of nine γ rays from four resonances show that a significant correlation coefficient $\rho(\Gamma_{\gamma ij}, \Gamma_{ni}^0) = 0.54$ is obtained. As established by Lane (9) the existence of a correlation coefficient between resonances implies the presence of a background term in the capture cross section. Dr Chrien will discuss the ENL efforts for a search for this background cross section in the Dy and Yb region.

In a recent effort to search for nonstatistical effects, Jafa et al (49) made use of the method of integrated intensity ratio where the ratio of the total intensity of $E_\gamma > 5$ MeV to that for $E_\gamma < 1.5$ is obtained for each resonance. If one assumes that the low γ ray energy spectrum is constant, then

this ratio, R , gives a measure of $E\Gamma_{\gamma 1j}$. A significant correlation coefficient between R and r_{ni}^0 is reported for Tb. However, Ribon et al.⁽⁵⁰⁾ measured the γ ray spectra from individual resonances of Tb and their results do not substantiate the findings of Jain et al.⁴⁹ Such contradictory results exemplify the experimental problems associated with the determination of nonstatistical effects in this mass region.

IV SUMMARY

Reliable and extensive thermal and resonance capture spectra data are now available, which indicate that the capture process for low energy neutrons is not in complete accord with the extreme statistical model via compound nucleus formation as postulated by Bohr. Detailed examination of the thermal capture data, particularly for the odd isotopes, show that correlation coefficients approaching unity can be derived for reduction factors of the γ ray energy of either 1 or 2.5. These respective values are precisely what is expected from "direct" and channel valence capture, thus presenting one verification of the Lane and Lynn theory of capture. In resonance capture in the neighborhood of the 2p, 3p, and 3s giant resonances, quantitative calculations show that valence capture plays a significant and often a dominant role. In those cases where the magnitude of the valence component is inadequate to explain the correlations, doorway state processes are invoked. However, in contrast to the valence model, the doorway or 2 p-1h picture is still qualitative in nature. Detailed theoretical calculations and further experimental investigations are required in order to shed additional light on this fascinating field.

ACKNOWLEDGEMENTS

I am greatly indebted to A. M. Lane for stimulating correspondence, to E. H. Auerbach for computer assistance, and to B. A. Magurno for Figure 9.

REFERENCES

1. A. M. Lane in International Conference on Photoneuclear Reactions and Applications, Vol. 2, p. 803 edited by B. L. Berman.
2. S. F. Mughabghab in Nuclear Structure Study with Neutrons, p. 167 edited by J. Ero and J. X. Saucis (Plenum Press, N.Y. 1974).
3. J. Kopacky and A. M. J. Spits, RCN Report No. 74-055 (1974).
4. J. Kopacky, A. M. J. Spits and A. M. Lane Phys. Letters, 49B, (1974) 323.
5. A. M. Lane and J. E. Lynn Nucl. Phys. 17, (1960) 563, 586.
6. J. E. Lynn, The Theory of Neutron Resonance Reactions, p. 333 (Clarendon Press, Oxford, England, 1968).
7. J. E. Brown, Nucl. Phys. 57, (1964) 339.
8. L. Estrada and N. Feinberg, Ann. Phys. 23, (1963) 123.
9. A. M. Lane, Ann. Phys. 63 (1972) 171.
10. H. Beer, Ann. Phys. 65 (1971) 181.
11. A. M. Lane and S. F. Mughabghab, Phys. Rev. C, 10, (1974) 412.
12. E. Vogt, Rev. Mod. Phys. 34, (1962) 723.
13. S. F. Mughabghab, R. E. Chrien, O. A. Wasson, G. W. Cole, and M. R. Bhat, Phys. Rev. Letters 26 (1971) 1118.
14. A. M. Lane, Phys. Letters 50B, (1974) 204.
15. B. Gyarmati, A. M. Lane, J. Zimanyi, Phys. Letters, 50B, (1974) 316.
16. H. Boridy and C. Mahaux Nucl. Phys. A209 (1973), 604.
17. E. Boridy and C. Mahaux, Nucl. Phys. A215, (1973) 605.
18. L. V. Groshov, A. M. Demidov, V. L. Lutsenko, and V. I. Palekhov in Proceedings of the Second United Nations International Conference on the Peaceful Use of Atomic Energy, Geneva, Vol. 15, (1958) p. 138.
19. A. M. Lane and D. H. Wilkenson, Phys. Rev. 97, (1955) 1199.
20. C. K. Bohlsen, Nucl. Phys. 13, (1959), 205.
21. S. F. Mughabghab, Private Communication.
22. A. M. Lane in Proc. Symp. on Neutron Capture Gamma-Ray Spectroscopy Studsvik, August 1969, p. 531 (IAEA, Vienna, 1969).
23. A. M. J. Spits and J. A. Akkermans, Nucl. Phys., A215 (1973) 260.

23. S. F. Mughabghab and D. I. Garber, ENL-325, Volume 1, Resonance Parameters.
25. M. A. J. Mariscotti, J. A. Moragus, W. Galletly, and W. R. Kane, Phys. Rev. Letters 22, (1969) 303.
26. V. L. Groshev, V. N. Dvoretckii, A. M. Demidov, and M. S. Alvash, Yad. Fiz. 10, (1969) 681.
27. I. Berqvist, J. A. Siggerstaff, J. H. Gibbons, and W. M. Good, Phys. Rev. 158, (1967), 1049.
28. K. J. Eglan, C. D. Bowman, and B. L. Berman, Phys. Rev. C, 3, (1971) 672.
29. S. F. Mughabghab in International Conference on Photoneuclear Reactions and Applications, 1, p. 301 (1973) (edited by B. L. Berman).
30. H. E. Jackson and R. E. Toohey, Phys. Rev. Letters, 29, (1972) 379.
31. B. J. Allen and R. L. Machlin, *ibid* reference (1) Volume 1, p. 291.
32. M. E. Chrien, A. P. Jain and H. Palevsky, Phys. Rev. 125, (1962) 275.
33. Von F. Wille, Atomkernenergie 13, (1968) 383 and Private Communication.
34. S. F. Mughabghab, Physics Letters 35B, (1971) 469.
35. J. Kopecky, K. Abrahams and F. Stecher-Rasmussen, Nucl. Phys. A188, (1972), 535.
36. R. G. Stieglitz, R. W. Hockenberry, and R. C. Block, Nucl. Phys. A163, (1971) 592.
37. R. R. Spencer and H. Beer, Private Communication.
38. O. A. Wasson and G. G. Slaughter, Phys. Rev. C, 8, (1973) 297.
39. K. Rimawi and R. E. Chrien, Bull. Am. Phys. Soc. 19 (1974) 9 and Private Communication.
40. K. Rimawi, R. E. Chrien, J. B. Garg, M. R. Bhat, D. I. Garber and O. A. Wasson, Phys. Rev. Lett. 23, (1969), 1041.
41. M. E. Toohey and H. E. Jackson, Phys. Rev. C, 9, (1974) 346.
42. S. F. Mughabghab, W. R. Kane and R. F. Casten, Contribution (D-2) to the Conf. on Nuclear Structure Study with Neutrons, Budapest 1972.
43. M. A. Lons, R. E. Chrien, O. A. Wasson, M. Beer, M. R. Bhat, and H. R. Muether, Phys. Rev. 174, (1968), 1512.

44. S. F. Mughabghab, R. E. Chrien, and O. A. Wasson, Phys. Rev. Letters 25, (1970) 1670.
45. O. A. Wasson, S. F. Mughabghab, and R. E. Chrien, Bull. Am. Phys. Soc. 16, (1971) 496.
46. B. W. Thomas in Statistical Properties of Nuclei, Edited J. B. Garg, (Plenum Press, New York-London 1972) p. 251.
47. L. S. Danelyan et al Zh. Exprim i. Theoret. Fiz. 62 (1972) 25.
48. G. C. Slaughter, O. A. Wasson, S. F. Mughabghab, R. E. Chrien, G. W. Cole, M. R. Bhat, Bull. Am. Phys. Soc. 17, (1972) 580.
49. A. P. Jain, B. Cauvin, and H. Lottin, Nucl. Phys. A223, (1974) 509.
50. P. Ribon, R. E. Chrien, G. W. Cole, Bull. Am. Phys Soc. 18, (1973), 1402.